analytically MHD nanofluid flow in a non parallel channel. Nano fluid flow and heat transfer in an asymmetric porous channel with expanding and contracting wall was studied numerically by Hatami, Sheikholeslami, and Ganji (2014), Mallikarjuna, Rashad, Chamkha, and Hariprasad (2016) investigated MHD flow of an incompressible viscous fluid from a rotating vertical cone in porosity regime. Mohammadreza and Rouzbeh (2016) investigated MHD copper-water nanofluid flow and heat transfer through a convergent-divergent channel. Umarkhan, Naveed, and Syed (2015) presented heat and mass transfer analysis for viscous incompressible fluid in converging and diverging channel and studied Soret and Dufour effects. Fakour, Vahabzadeh, Ganji, and Hatami (2015) investigated analytically heat transfer of a micropolar fluid in a channel with penetrable walls. Ghadikolaei, Hosseinzadeh, Yassari, Sadeghi, and Ganji (2018) studied second grade fluid flow on a streching sheet analytically and compared the result with numerical solution.

Two-phase flow of particulate suspension applications abound in many areas of technology: food industries, powder technology, waste water treatment, combustion and corrosive particles in engine oil flow etc. So it is important to study fluid-particle hydromagnetic convective flows in order to understand the influence of the different phases on heat transfer processes. Recently, a remarkable number of researchers, Sivakumar, Sreenath, and Pushpavanam (2010), Hatami, Hosseinzadeh, Domairry, and Behnamfar (2014) have investigated two-phase particulate flows with and without magnetic field and heat transfer analytically and numerically. Chamkha (1995) studied hydromagnetic two-phase flow in a channel. Mansour and Chamkha (2003) developed a continuum model to analyze heat generation effects on two-phase particulate suspension MHD flow through a channel. Usha, Senthilkumar, and Tulapurkara (2006) investigated particulate suspension flow in a travelling wavy channel. Heat generation effects on hydromagnetic flow of a particulate suspension through isothermal-isoflux channels was investigated by Chamkha and Rashidi (2010). Rawat *et al*. (2014) presented a numerical model for steady two dimensional two-phase hydromagnetic flows and heat transfer in a particulate-suspension through a non-Darcian porous channel. Sadia, Naheed, and Anwar (2017) studied compressible dusty gas along a vertical wavy surface. Krupalakshmi, Gireesha, Gorla, and Mahanthesh (2016) investigated numerically laminar boundary layer flowheat and mass transfer of two-phase particulate suspension past a stretching sheet with chemical reaction. Mohammad, Islam, Prilal, Ramzan, and Abumandown (2015) investigated peristaltic transport of a particle-fluid suspension in a planar channel by taking slip effects on the wall into account. Eldesoky, Abdelsalam, Abumandown, Kamel, and Vafai (2017) analytically studied interaction between compressibility and particulate suspension on peristaltically driven flow in a planar channel. Mallikarjuna, Rashad, Hussein, and Hariprasad (2016) studied numerically the effects of transpiration, thermal radiation and thermophoresis effects on convective flow over a rotating cone in a non-Darcy porous medium. Recently Ramprasad, Subba Bhatta, and Mallikarjuna (2018) considered velocity and temperature slip effects and studied numerically particulate suspension flow in a divergent channel.

With the available literature and to the best of the authors knowledge, no one has studied convective two-phase flow in an asymmetric divergent channel. Keeping in view the above facts, a mathematical model has been developed to study MHD convective two-phase particulate suspension flow in a divergent channel with heat source.

2. Model of the Problem

Consider steady, viscous, two-dimensional incompressible laminar two-phase flow of particulate suspension in an asymmetric diverging channel. Walls of the channel are placed at $\theta = \pm\alpha$ as shown in Figure 1. Suction/injection velocities are assumed at different walls and these velocities are to be varied inversely proportional to the distance along the wall from origin of the channel. The continuity equation, the Navier–Stokes equations and the energy equation governing the flow in polar coordinates (r,θ) are given by Terril (1965) and Baris (2003)

For fluid phase

$$\frac{\partial}{\partial r}(ru)+\frac{\partial v}{\partial \theta}=0, \tag{1}$$

$$\left(u\frac{\partial u}{\partial r}+\frac{v}{r}\frac{\partial u}{\partial \theta}-\frac{v^2}{r}\right)=-\frac{1}{\rho}\frac{\partial p}{\partial r}+\upsilon\left[\left(\frac{\partial^2 u}{\partial r^2}+\frac{1}{r}\frac{\partial u}{\partial r}+\frac{1}{r^2}\frac{\partial^2 u}{\partial \theta^2}\right)-\frac{u}{r^2}+\frac{2}{r^2}\frac{\partial v}{\partial \theta}\right]+\frac{\rho_p}{\rho}S\left(u_p-u\right)-\frac{\sigma H_0^{\,2}\mu_e^{\,2}u}{\rho}-g\beta^* T, \tag{2}$$

$$\left(u\frac{\partial v}{\partial r}+\frac{v}{r}\frac{\partial v}{\partial \theta}+\frac{uv}{r}\right)=-\frac{1}{\rho r}\frac{\partial p}{\partial \theta}+\upsilon\left[\left(\frac{\partial^2 v}{\partial r^2}+\frac{1}{r}\frac{\partial v}{\partial r}+\frac{1}{r^2}\frac{\partial^2 v}{\partial \theta^2}\right)-\frac{v}{r^2}+\frac{2}{r^2}\frac{\partial u}{\partial \theta}\right]+\frac{\rho_p}{\rho}S\left(v_p-v\right), \tag{3}$$

$$u\frac{\partial T}{\partial r}+\frac{v}{r}\frac{\partial T}{\partial \theta}=\frac{k}{\rho c_p}\left(\frac{1}{r}\frac{\partial}{\partial r}\left(r\frac{\partial T}{\partial r}\right)+\frac{1}{r^2}\frac{\partial^2 T}{\partial \theta^2}\right)+\frac{Q_0}{\rho c_p}T+\frac{\rho_p C_m}{\tau_T \rho c_p}\left(T_p-T\right), \tag{4}$$

For particle phase

$$\frac{\partial}{\partial r}\left(ru_p\right)+\frac{\partial v_p}{\partial \theta}=0, \tag{5}$$

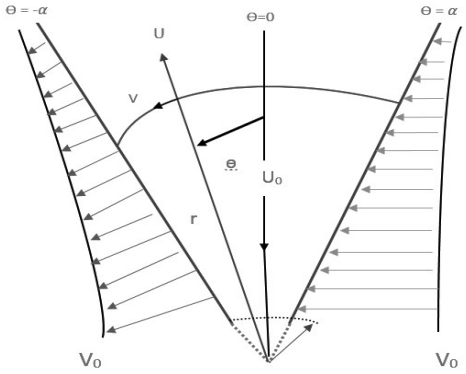

Figure 1. Geometry of the flow

$$\left(u_p\frac{\partial u_p}{\partial r}+\frac{v_p}{r}\frac{\partial u_p}{\partial \theta}-\frac{v_p^{\,2}}{r}\right)=-\frac{1}{\rho_p}\frac{\partial p}{\partial r}+S\left(u-u_p\right)-g\beta^{*}T_p, \tag{6}$$

$$\left(u_p\frac{\partial v_p}{\partial r}+\frac{v_p}{r}\frac{\partial v_p}{\partial \theta}+\frac{u_pv_p}{r}\right)=-\frac{1}{r\rho_p}\frac{\partial p}{\partial \theta}+S\left(v-v_p\right), \tag{7}$$

$$u_p\frac{\partial T_p}{\partial r}+\frac{v_p}{r}\frac{\partial T_p}{\partial \theta}=\frac{1}{\tau_T}\left(T-T_p\right), \tag{8}$$

The associated boundary conditions are

$$\begin{aligned}&u=0,u_p=0\quad at\,\theta=\pm\alpha\quad u\left(\theta=0\right)=U_0\\&T=T_w,T_p=T_{w_p}\,at\;\theta=\pm\alpha\end{aligned} \tag{9}$$

Introducing the following dimensionless variables

$$u=\frac{U_0r_0f\left(\theta\right)}{r};u_p=\frac{U_0r_0g\left(\theta\right)}{r};v_p=\frac{V_{p_0}r_0}{r};v=\frac{V_0r_0}{r};\;h=\frac{T}{T_w};\;H=\frac{T}{T_{w_p}}$$

Equation $(1)-(9)$ are reduced to

$$f'''+2\mathrm{Re}\,ff''-Rf''+L\beta\left(g'-f'\right)+\left(4-M^2\right)f'-\frac{Gr}{\mathrm{Re}}h'=0, \tag{10}$$

$$g''-2\frac{\mathrm{Re}}{R}gg'-\frac{\beta}{R}\left(f'-g'\right)-\frac{Gr}{\mathrm{Re}\,R}H'=0, \tag{11}$$

$$h''-RPrh'+PrQh+L\beta_t\gamma Pr\left(H-h\right)=0, \tag{12}$$

$$H'-K\left(h-H\right)=0\,, \tag{13}$$

Associated boundary conditions are

$$\begin{aligned}&f\left(\pm\alpha\right)=0,f'\left(0\right)=1\\&g\left(\pm\alpha\right)=0,h\left(\pm\alpha\right)=1,H\left(\pm\alpha\right)=1\end{aligned} \tag{14}$$

3. Skin Friction Coefficient and Nusselt Number

The main aim of the physical interest of the problem is analyzing drag coefficient and rate of heat transfer over surface of the channel, which are defined by skin friction

$$C_f=\frac{\tau_s}{\rho U_o^2}=\frac{\mu\left(\dfrac{\partial u}{r\partial\theta}\right)_{\theta=\pm\alpha}}{\rho U_o^2}$$ and Nusselt number

$$Nu=\frac{rq_s}{\kappa T_w}=\frac{r\left(\dfrac{-\kappa\partial T}{r\partial\theta}\right)_{\theta=\pm\alpha}}{\kappa T_w}$$

In non-dimensional form

$$C_f=\frac{1}{\mathrm{Re}}f'\left(\pm\alpha\right)\text{ and }Nu=-h'\left(\pm\alpha\right)$$

4. Solution Methodology

A set of equations $(10)-(13)$ with boundary con-ditions (14) are first rewritten in a system of first order equations by assuming $f=f(1),f'=f(2),f''=f(3),\;g=f(4),g'=f(5),h=f(6),\;h'=f(7),H=f(8),\;\;H'=f(9)$, i.e.

$$\frac{dY}{dx}=\frac{d}{dx}\begin{bmatrix}f(1)\\f(2)\\f(3)\\f(4)\\f(5)\\f(6)\\f(7)\\f(8)\\f(9)\end{bmatrix}=\begin{bmatrix}f(2)\\f(3)\\f'''=-2\mathrm{Re}\,f(1)f(2)+Rf(3)-L\beta\left(f(5)-f(2)\right)-\left(4-M^2\right)f(2)+\dfrac{Gr}{\mathrm{Re}}f(7)\\f(5)\\g''=2\dfrac{\mathrm{Re}}{R}f(4)f(5)+\dfrac{\beta}{R}\left(f(2)-f(5)\right)+\dfrac{Gr}{\mathrm{Re}\,R}f(9)\\f(7)\\h''=R\,\mathrm{Pr}\,f(7)-\mathrm{Pr}Qf(6)-L\beta_t\,\mathrm{Pr}\,\gamma\left(f(8)-f(6)\right)\\f(9)\\H''=K\left(f(7)-f(9)\right)\end{bmatrix} \tag{15}$$

We choose some initial conditions $f'\left(-\alpha\right)=c_1,f''\left(-\alpha\right)=c_2,g'\left(-\alpha\right)=c_3,\;h'\left(-\alpha\right)=c_4,$ and $H'\left(-\alpha\right)=c_5$ which are not given at initial point and integrate (15) using Runge-Kutta fourth order technique (Ghadikolaei, Hosseinzadeh, & Ganji, 2018;

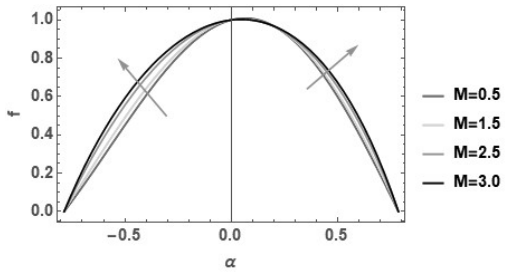

Figure 2. Effect of M on fluid phase velocity

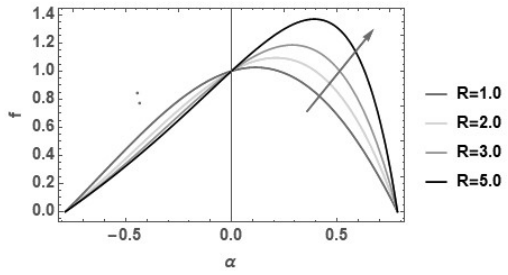

Figure 3. Effect of R on fluid phase velocity

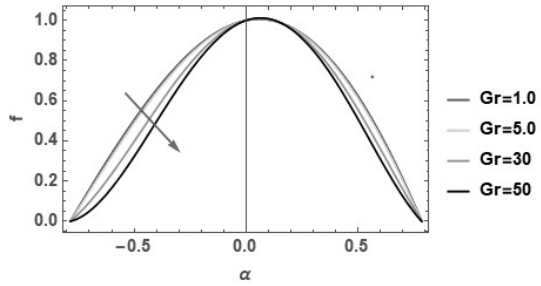

Figure 4. Effect of Gr on fluid phase velocity

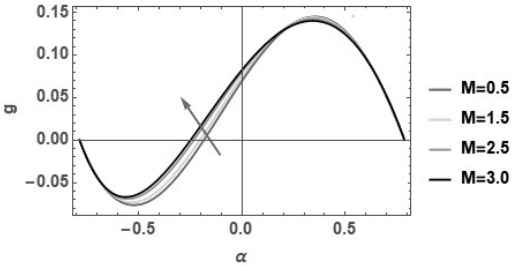

Figure 5. Effect of M on particle phase velocity

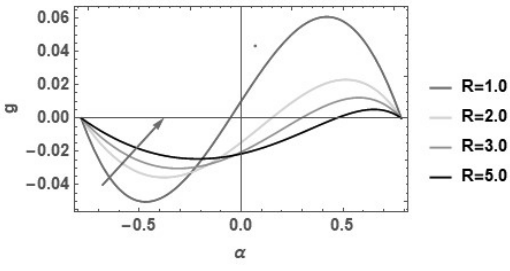

Figure 6. Effect of R on particle phase velocity;

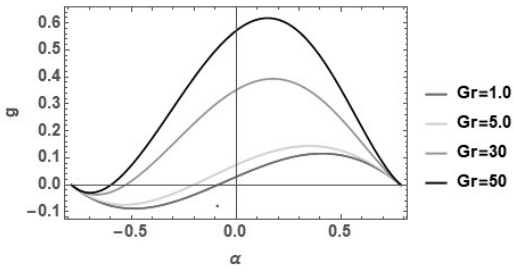

Figure 7. Effect of Gr on particle phase velocity

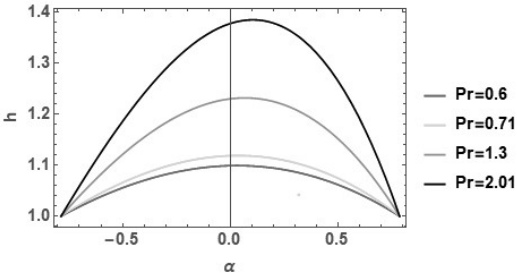

Figure 8. Effect of Pr on fluid phase temperature

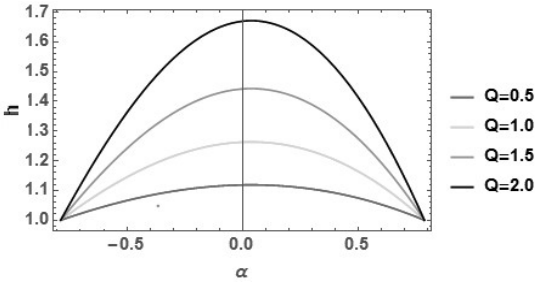

Figure 9. Effect of Q on fluid phase temperature

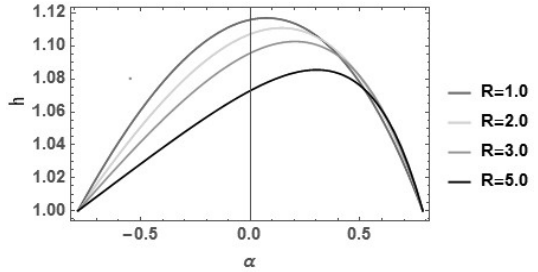

Figure 10. Effect of R on fluid phase temperature

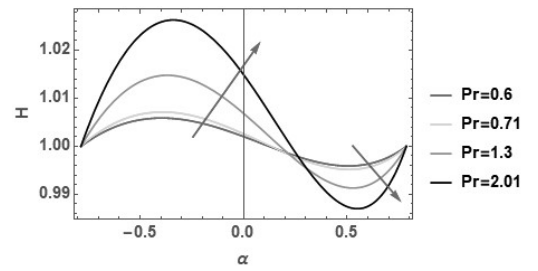

Figure 11. Effect of Pr on particle phase temperature